PHYSICAL REVIEW A **81**, 020305(R) (2010)

Ultrafast control of nuclear spins using only microwave pulses: Towards switchable solid-state quantum gates

George Mitrikas,* Yiannis Sanakis, and Georgios Papavassiliou
Institute of Materials Science, NCSR Demokritos, GR-15310 Athens, Greece
(Received 13 October 2009; published 24 February 2010)

We demonstrate the control of the α-proton nuclear spin, $I = 1/2$, coupled to the stable radical $\cdot CH(COOH)_2$, $S = 1/2$, in a γ-irradiated malonic acid single crystal using only microwave pulses. We show that, depending on the state of the electron spin ($m_S = \pm 1/2$), the nuclear spin can be locked in a desired state or oscillate between $m_I = +1/2$ and $m_I = -1/2$ on the nanosecond time scale. This approach provides a fast way of controlling nuclear spin qubits and also enables the design of switchable spin-based quantum gates by addressing only the electron spin.

DOI: 10.1103/PhysRevA.81.020305 PACS number(s): 03.67.Lx, 76.60.−k, 76.30.−v

Since the idea of quantum information processing (QIP) began fascinating the scientific community [1–3], electron and nuclear spins have been regarded as promising candidates for quantum bits (qubits) [4]. Nuclear magnetic resonance (NMR) in liquid state was the first spectroscopic technique used to demonstrate several quantum computation algorithms [5–8], while some of the emerged scalability limitations can be overcome by using electron paramagnetic resonance (EPR) spectroscopy [9]. The construction of quantum gates based exclusively on electron spins with controllable exchange interactions is, however, a challenging task, especially when crystalline materials of this kind are on demand. This difficulty has motivated an on-going effort to find appropriate electron spin qubits, including, for instance, quantum dots [10], single-molecule magnets [11], and antiferromagnetic heterometallic rings [12] or metal clusters [13]. On the other hand, hybrid electron-nuclear spin systems with long decoherence times can be found in a variety of materials such as organic single crystals [14], endohedral fullerenes [15–17], phosphorous donors in silicon crystals [18], and nitrogen-vacancy centers in diamond [19,20]. They have been used to perform two-qubit quantum operations, demonstrate entangled states, or build solid-state quantum memories. These systems benefit from well-defined and separated EPR and NMR transitions that can be selectively manipulated by resonant microwave (mw) and radio frequency (rf) radiation, respectively. Therefore, advanced EPR methods [21] employing both selective mw and rf pulses play a key role in QIP based on electron-nuclear spin systems.

The significant difference between decoherence times of electron (T_{2e}) and nuclear (T_{2n}) spins, which is due to the fact that their gyromagnetic ratios γ_i differ by two to three orders of magnitude, has been utilized for the realization of a quantum memory that uses slow relaxing nuclear spins to store the information and fast relaxing electron spins for processing and readout [18]. On the other hand, this difference also restricts the clock rates of gate operation to the corresponding ones of the slow relaxing qubit, namely, to the MHz frequency scale. More seriously, though, the combination of the small gyromagnetic ratios γ_n of nuclei with the currently available rf fields B_1 results in slow rotations of nuclear spins. For instance, the nutation (Rabi) frequency of a proton nuclear spin for a typical value of $B_1 = 1$ mT is $\omega_1/2\pi = \gamma_n B_1/h = 42.6$ kHz, which implies a length of $\Delta t_\pi = 11.7$ μs for an rf π pulse. This time interval is of the same order of magnitude as with typical electron decoherence times T_{2e}, and thus the efficiency of the two-qubit quantum gate may become questionable due to relaxation losses.

One way to overcome this difficulty is to utilize the hyperfine interaction which is typically stronger than the Rabi nuclear frequency, i.e., of the order of some MHz in organic radicals. When this interaction is anisotropic, the quantization axes of the hyperfine fields deviate from the z axis [see Fig. 1(a)], and thus the nutating nuclear spin can be inverted by implementing a proper set of mw π pulses separated by suitable time delays [22]. This concept has been recently used in a similar fashion [23] to demonstrate the creation of nuclear spin coherence via amplitude-modulated mw pulses [24].

Herein we focus on a special case of electron spin echo envelope modulation (ESEEM) spectroscopy, the so-called exact cancellation [21] where the hyperfine and nuclear Zeeman interactions cancel each other in one m_S manifold.

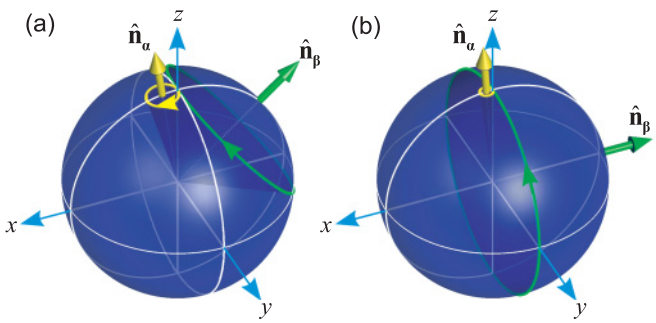

FIG. 1. (Color online) (a) Bloch sphere showing the trajectories of nuclear-spin magnetization under free evolution assuming that the nuclear spin is polarized in the beginning ($m_I = +1/2$). The quantization axis of the effective magnetic field experienced by the nucleus depends on the state of the electron spin: for $m_S = +1/2$, the nuclear spin precesses about $\hat{\boldsymbol{n}}_{\boldsymbol{\alpha}}$ (yellow trace) with angular frequency $\omega_\alpha = |\omega_{12}|$; for $m_S = -1/2$, the nuclear spin precesses about $\hat{\boldsymbol{n}}_{\boldsymbol{\beta}}$ (green trace) with angular frequency $\omega_\beta = |\omega_{34}|$. (b) Exact cancellation case, $\omega_I = A/2$.

*mitrikas@ims.demokritos.gr

Figure 1(b) shows that in this case the effective magnetic field at the nucleus is either almost parallel or exactly perpendicular to the z axis, depending on the state of the electron spin. Consequently, during free evolution of the system with $m_S = -1/2$, the nuclear spin naturally oscillates between the $m_I = +1/2$ and $m_I = -1/2$ states without the need of an rf field. In addition, it can be locked in a desired state by inverting the electron spin state to $m_S = +1/2$ with a mw π pulse applied after a proper time delay.

To demonstrate this control, a single crystal of γ-irradiated malonic acid is used. Here the paramagnetic species is the stable radical $\cdot CH(COOH)_2$ shown in Fig. 2(a), where the unpaired electron ($S = 1/2$) resides on the carbon $2p_z$ orbital and is hyperfine-coupled to the α-proton nuclear spin ($I = 1/2$) [25]. The rotating frame spin Hamiltonian is given by [21]

$$\mathcal{H}_0 = \Omega_S S_z + \omega_I I_z + A S_z I_z + B S_z I_x, \qquad (1)$$

where $\Omega_S = \omega_S - \omega_{\rm mw}$ is the offset of the electron Zeeman frequency $\omega_S = g\beta_e B_0/\hbar$ from the mw frequency $\omega_{\rm mw}$, $\omega_I = -g_n\beta_n B_0/\hbar$ is the nuclear Zeeman frequency, g and g_n are the electron and nuclear g factors, β_e and β_n are the Bohr and nuclear magnetons, B_0 is the static magnetic field along the z axis, and A, B describe the secular and pseudosecular part of the hyperfine coupling. In this four-level electron-nuclear spin system [Fig. 2(b)], there are six possible transitions: four EPR with $\Delta m_S = \pm 1$, as illustrated in the stick spectrum of Fig. 2(c), and two NMR with frequencies ω_{12} and ω_{34}. For a proton nuclear spin ($\omega_I < 0$) and a negative hyperfine coupling ($A < 0$) in the weak-coupling regime ($|A| < 2|\omega_I|$), the singed nuclear transition frequencies can be expressed as $\omega_{12} = -\sqrt{(\omega_I + A/2)^2 + (B/2)^2}$ and $\omega_{34} = -\sqrt{(\omega_I - A/2)^2 + (B/2)^2}$. In addition, the quantization axes of the effective frequency vectors are determined by the angles $\eta_\alpha = \arctan[-B/(A + 2\omega_I)]$ and $\eta_\beta = \arctan[-B/(A - 2\omega_I)]$, which are defined relative to the z direction. For the case of interest of exact cancellation, $A = 2\omega_I$, the nuclear transition frequencies become $\omega_{12} = -\sqrt{(2\omega_I)^2 + (B/2)^2}$ and $\omega_{34} = -B/2$ (with $B > 0$) with

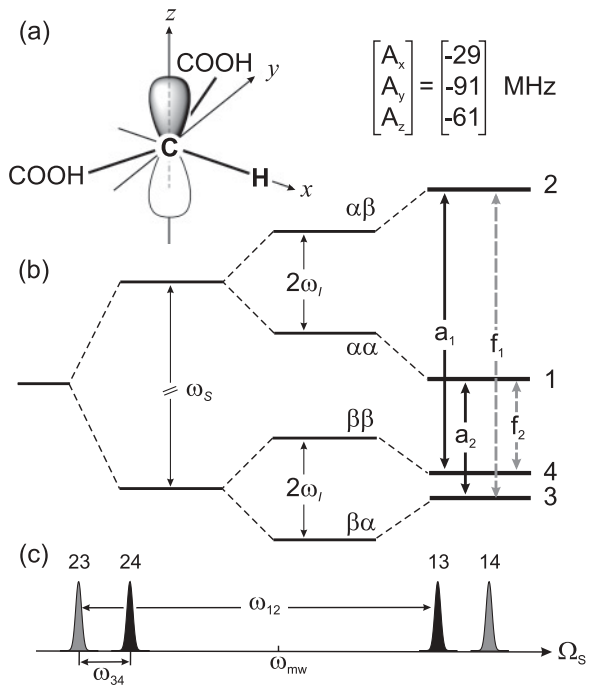

FIG. 2. (a) Schematic representation of the stable radical $\cdot CH(COOH)_2$ and the principal axes system of the hyperfine tensor. (b) Energy level diagram depicting the allowed (a1, a2) and forbidden (f1, f2) electron spin transitions. (c) EPR stick spectrum.

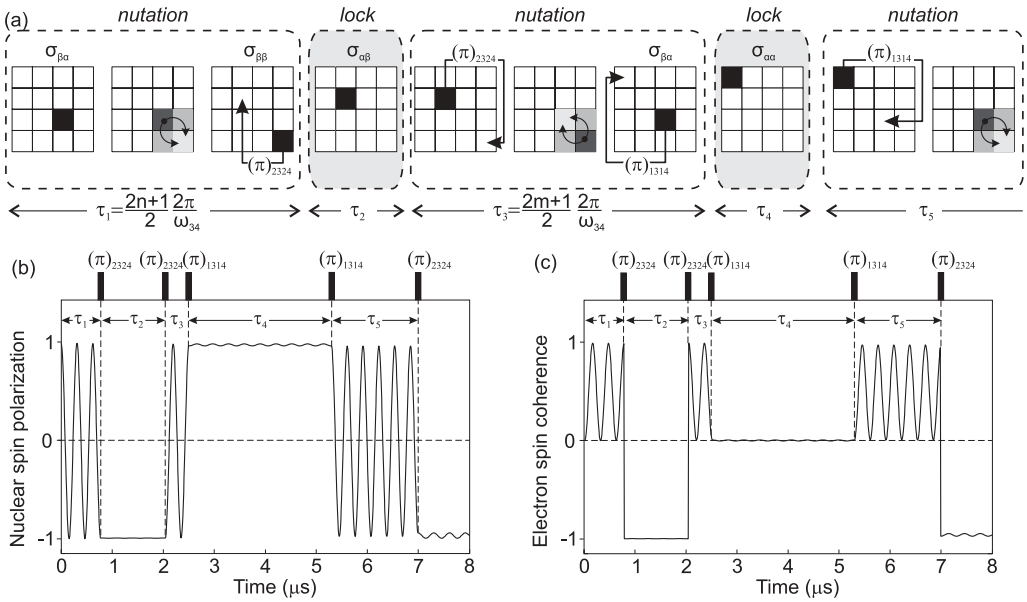

FIG. 3. (a) Representation of the density matrix in the product basis $|\alpha\alpha\rangle$, $|\alpha\beta\rangle$, $|\beta\alpha\rangle$, $|\beta\beta\rangle$ during nutation or locking time periods. (b) Numerical simulation of the nuclear spin polarization $\langle I_z\rangle$ during the applied pulse sequence that uses semiselective mw π pulses (shown at the top). Spin Hamiltonian parameters: nuclear Zeeman frequency, $\omega_I/2\pi = -14.58$ MHz; hyperfine coupling constants, $A/2\pi = -29.06$ MHz, $B/2\pi = 6.45$ MHz. (c) Corresponding numerical simulation of the electron spin coherence $\langle S_x\rangle$ after the detection pulse sequence $(\pi/2)_{2324} - \tau - (\pi)_{2324} - \tau -$ echo with $\tau = 2\pi/\omega_{34} = 310$ ns.

the corresponding angles being $\eta_\alpha = \arctan[-B/4\omega_I]$ and $\eta_\beta = -\pi/2$.

The concept of manipulating the proton nuclear spin solely by using mw pulses can be best described in terms of the density matrix formalism. Figure 3(a) shows an example of this control assuming that the system is initially prepared in the pseudopure state $\sigma_{\beta\alpha} \equiv |\beta\alpha\rangle\langle\beta\alpha|$, which is described by the density matrix in the product basis

$$\sigma_{\beta\alpha} = \begin{pmatrix} 0 & 0 & 0 & 0 \\ 0 & 0 & 0 & 0 \\ 0 & 0 & 1 & 0 \\ 0 & 0 & 0 & 0 \end{pmatrix}.$$

During free evolution of the system under the spin Hamiltonian [Eq. (1)] the hyperfine field drives the nuclear spin transition, and the population is periodically transferred from $\sigma_{\beta\alpha}$ to $\sigma_{\beta\beta}$ and vice versa with frequency ω_{34}. This transfer is complete (i.e., $\sigma_{\beta\beta} \equiv |\beta\beta\rangle\langle\beta\beta|$) only if the exact cancellation condition $\sin\eta_\beta = -1$ is fulfilled, and occurs for free evolution times $\tau_1 = (2m+1)\pi/\omega_{34}$ ($m = 0, 1, 2, \ldots$) [26] (see supplementary information). A subsequent semiselective mw π pulse, which simultaneously excites the forbidden 23 and allowed 24 EPR transitions [27,28] [represented as $(\pi)_{2324}$], transfers the population to the $|\alpha\beta\rangle$ state. Provided that the angle η_α is very small, the populations and nuclear coherences in the $m_S = +1/2$ subspace are virtually trapped because of the negligible branching between $|\alpha\alpha\rangle$ and $|\alpha\beta\rangle$ states. Under that treatment, the nuclear spin can be locked in the $m_I = -1/2$ state for arbitrary time τ_2. An additional $(\pi)_{2324}$ pulse will transfer the population back to the $|\beta\beta\rangle$ state, and the nuclear spin will start oscillating again between $m_I = +1/2$ and $m_I = -1/2$ with frequency ω_{34}. Quantitatively, this is demonstrated in Fig. 3(b), which shows the simulation of the nuclear spin polarization $\langle I_z\rangle$. Therefore, by choosing appropriate time delays and semiselective mw pulses, the full control of the nuclear spin can be achieved.

Although direct measurement of nuclear spin polarization is not possible in EPR spectroscopy, Fig. 3(c) shows that the electron spin coherence $\langle S_x\rangle$ after the sequence $(\pi/2)_{2324} - \tau - (\pi)_{2324} - \tau -$echo with $\tau = 2\pi m/\omega_{34}$ ($m = 1, 2, 3\ldots$) represents the population difference between states 2 and 4. Consequently, such a subsequence can be used to monitor the state of our system.

For the experimental demonstration of this control, the system can start from a pseudopure state, e.g., $\sigma_{\beta\alpha}$. For the case of isotropic hyperfine coupling ($B = 0$), such a state can be prepared with a selective mw pulse $P_{24}(\beta_0)$, with $\beta_0 = \arctan(-1/3) = 109.5^\circ$, followed by a $\pi/2$ rf pulse, $P_{12}(\pi/2)$ [4]. For anisotropic hyperfine coupling and a strong mixing of states, the above pulse sequence does not result in the desired pseudopure state. However, for the special case of exact cancellation, the operation of a selective mw pulse $P_{24}(\beta)$ [with effective rotation angle $\beta_{\text{eff}} = \arctan(-1/3) = 109.5^\circ$] at the thermal equilibrium density matrix, $\sigma_0 = -S_z$, gives the pseudopure state $\sigma_{\alpha\alpha}$ in good approximation [26] (see supplementary information). An additional semiselective $(\pi)_{1314}$ pulse applied after time $T_d > 5T_{2e}$ complements the preparation part of the pulse scheme shown in Fig. 4(a) and leads the system to the pseudopure state $\sigma_{\beta\alpha}$.

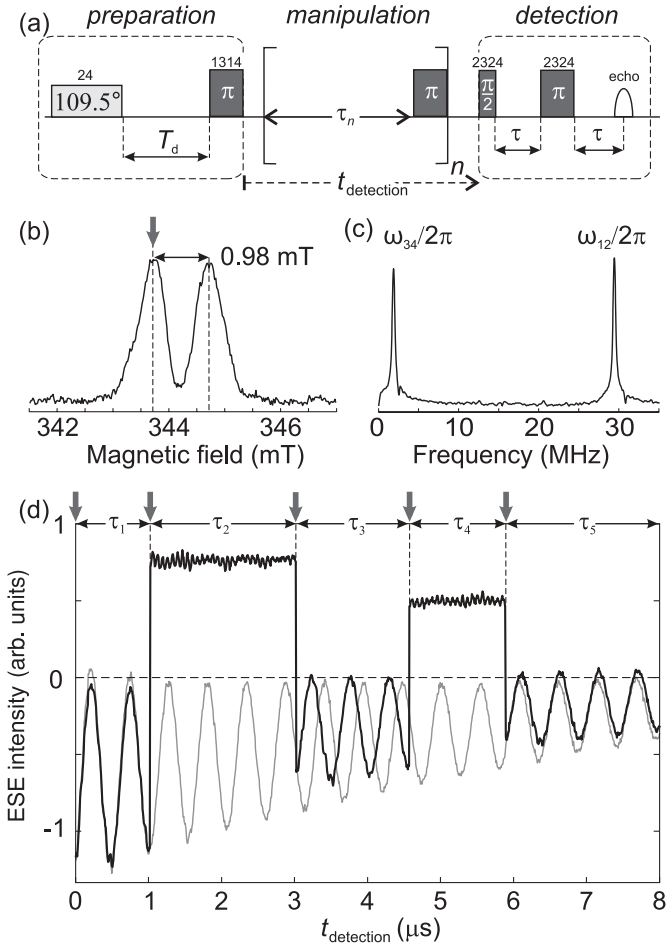

FIG. 4. (a) Proposed pulse sequence consists of three parts: preparation, for creating the pseudopure state $\sigma_{\beta\alpha}$; manipulation, consisting of a time delay τ_n and a semiselective $(\pi)_{2324}$ or $(\pi)_{1314}$ pulse; detection of electron-spin coherence through a two-pulse echo with $\tau = 2\pi/\omega_{34}$. (b) Free induction decay (FID)-detected EPR spectrum. The arrow indicates the observer position $B_0 = 343.7$ mT of the semiselective $(\pi)_{2324}$ pulses. (c) Three-pulse ESEEM spectrum. (d) Electron spin echo (ESE) intensity as a function of time $t_{\text{detection}}$ between preparation and detection.

The experiments were performed at a crystal orientation for which the hyperfine coupling is very close to exact cancellation: the three-pulse ESEEM spectrum [Fig. 4(c)] measured at the observer position $B_0 = 343.7$ mT ($\omega_I/2\pi = -14.6$ MHz) shows two peaks at frequencies $\omega_{12}/2\pi = -29.42$ MHz and $\omega_{34}/2\pi = -1.83$ MHz from which the angles $\eta_\alpha = -3.6^\circ$ and $\eta_\beta = -87.1^\circ$ can be inferred. Figure 4(b) shows that the two EPR transitions 23 and 24 are not resolved due to the small nuclear frequency ω_{34} and inhomogeneous broadening. Therefore, an accurate excitation of transition 24 with a selective P_{24} pulse is difficult to accomplish. Moreover, the necessity of the semiselective $(\pi)_{1314}$ pulse requires an additional mw frequency that was not available with the current experimental setup. However, both technical issues were circumvented by replacing the preparation part of Fig. 4(a) with a semiselective $(\pi)_{2324}$ pulse that interchanges populations between levels 2 and 4. Their population difference (which is our observable here) is expected to oscillate between zero and a maximum

value, because after the semiselective pulse, levels 3 and 4 will start exchanging populations, in analogy with the situation of population transfer during the free evolution of $\sigma_{\beta\alpha}$ under the spin Hamiltonian [Eq. (1)]. Figure 4(d) (gray trace) shows that the signal virtually vanishes for $t = (m + 1/2)T$ ($m = 0, 1, 2, \ldots$), where $T = 504$ ns ($\approx 2\pi/\omega_{34}$), implying that our system is indeed very close to exact cancellation. By applying semiselective mw pulses, the nuclear-spin evolution can be locked in the $m_I = -1/2$ state or released at will [Fig. 4(d), black trace].

In conclusion, we have demonstrated that our approach provides a fast way of controlling nuclear spins in hybrid spin systems and thus overcomes the problem of relaxation incompatibility between electron and nuclear spins. Furthermore, the method offers a means for controlling the interaction between the two qubits in a fast and efficient way. Although the hyperfine interaction is always present, the special case of exact cancellation considered here induces two different effective states of interaction regarding the behavior of the nuclear spin: an active (nutation) and a passive (lock) state, which can be switched with a single mw pulse. While the control of dipolar interactions between neighboring electron spin qubits has been proposed using SWAP operations [29,30], to the best of our knowledge to date this kind of control in similar spin systems has been experimentally demonstrated only once using decoupling methods [31]. Our work shows that advanced pulsed EPR methods like ESEEM spectroscopy can play a key role in QIP based on hybrid electron-nuclear spin systems. Furthermore, it gives broader perspective to such systems by considering them not only for performing quantum memories but also for building solid-state quantum gates.

[1] D. Deutsch, Proc. R. Soc. London A **400**, 97 (1985).
[2] D. Deutsch and R. Jozsa, Proc. R. Soc. London A **439**, 553 (1992).
[3] C. H. Bennett and D. P. DiVincenzo, Nature (London) **404**, 247 (2000).
[4] M. Mehring, J. Mende, and W. Scherer, Lect. Notes Phys. **684**, 87 (2006).
[5] N. A. Gershenfeld and I. L. Chuang, Science **275**, 350 (1997).
[6] K. Dorai, Arvind, and A. Kumar, Phys. Rev. A **61**, 042306 (2000).
[7] J. Kim, J.-S. Lee, and S. Lee, Phys. Rev. A **65**, 054301 (2002).
[8] L. M. K. Vandersypen, M. Steffen, G. Breyta, C. S. Yannoni, M. H. Sherwood, and I. L. Chuang, Nature (London) **414**, 883 (2001).
[9] W. S. Warren, N. Gershenfeld, and I. Chuang, Science **277**, 1688 (1997).
[10] D. Loss and D. P. DiVincenzo, Phys. Rev. A **57**, 120 (1998).
[11] C. Schlegel, J. van Slageren, M. Manoli, E. K. Brechin, and M. Dressel, Phys. Rev. Lett. **101**, 147203 (2008).
[12] G. A. Timco, E. J. L. McInnes, R. G. Pritchard, F. Tuna, and R. E. P. Winpenny, Angew. Chem., Int. Ed. Engl. **47**, 9681 (2008).
[13] G. Mitrikas, Y. Sanakis, C. Raptopoulou, G. Kordas, and G. Papavassiliou, Phys. Chem. Chem. Phys. **10**, 743 (2008).
[14] M. Mehring, J. Mende, and W. Scherer, Phys. Rev. Lett. **90**, 153001 (2003).
[15] W. Scherer and M. Mehring, J. Chem. Phys. **128**, 052305 (2008).
[16] B. Naydenov, J. Mende, W. Harneit, and M. Mehring, Phys. Status Solidi B **245**, 2002 (2008).
[17] J. J. L. Morton, A. M. Tyryshkin, A. Ardavan, K. Porfyrakis, S. A. Lyon, and G. A. D. Briggs, Phys. Rev. B **76**, 085418 (2007).
[18] J. J. L. Morton *et al.*, Nature (London) **455**, 1085 (2008).
[19] L. Childress, M. V. G. Dutt, J. M. Taylor, A. S. Zibrov, F. Jelezko, J. Wrachtrup, P. R. Hemmer, and M. D. Lukin, Science **314**, 281 (2007).
[20] F. Jelezko, T. Gaebel, I. Popa, M. Domhan, A. Gruber, and J. Wrachtrup, Phys. Rev. Lett. **93**, 130501 (2004).
[21] A. Schweiger and G. Jeschke, *Principles of Pulse Electron Paramagnetic Resonance* (Oxford University Press, New York, 2001).
[22] N. Khaneja, Phys. Rev. A **76**, 032326 (2007).
[23] J. S. Hodges, J. C. Yang, C. Ramanathan, and D. G. Cory, Phys. Rev. A **78**, 010303(R) (2008).
[24] N. Khaneja, T. Reiss, C. Kehlet, T. Schulte-Herbruggen, and S. J. Glaser, J. Magn. Reson. **172**, 296 (2005).
[25] A. Horsfield, J. R. Morton, and D. H. Whiffen, Mol. Phys. **4**, 327 (1961).
[26] See supplementary material at http://link.aps.org/supplemental/10.1103/PhysRevA.81.020305 for theoretical description and experimental details.
[27] E. C. Hoffmann, M. Hubrich, and A. Schweiger, J. Magn. Reson. A **117**, 16 (1995).
[28] R. Rakhmatullin, E. Hoffmann, G. Jeschke, and A. Schweiger, Phys. Rev. A **57**, 3775 (1998).
[29] D. Suter and K. Lim, Phys. Rev. A **65**, 052309 (2002).
[30] C. Y. Ju, D. Suter, and J. F. Du, Phys. Rev. A **75**, 012318 (2007).
[31] J. J. L. Morton, A. M. Tyryshkin, A. Ardavan, S. C. Benjamin, K. Porfyrakis, S. A. Lyon, and G. A. D. Briggs, Nature Physics **2**, 40 (2006).